Applied Mathematical Modelling 46 (2017) 116–125

Contents lists available at ScienceDirect

Applied Mathematical Modelling

journal homepage: www.elsevier.com/locate/apm

Extending the excluded volume for percolation threshold estimates in polydisperse systems: The binary disk system

Kelsey Meeks[a,b,*], Michelle L. Pantoya[b], Micah Green[c], Jordan Berg[b]

[a] Sandia National Laboratories, Albuquerque, NM 87123, USA
[b] Mechanical Engineering Department, Texas Tech University, Lubbock, TX 79409-1021, USA
[c] Chemical Engineering Department, Texas A&M University, College Station, TX 77843-3122, USA

ARTICLE INFO

Article history:
Received 17 January 2016
Revised 12 September 2016
Accepted 13 January 2017
Available online 20 January 2017

Keywords:
Percolation
Binary disks
Excluded volume
Percolation threshold estimates

ABSTRACT

For dispersions containing a single type of particle, it has been observed that the onset of percolation coincides with a critical value of volume fraction. When the volume fraction is calculated based on excluded volume, this critical percolation threshold is nearly invariant to particle shape. The critical threshold has been calculated to high precision for simple geometries using Monte Carlo simulations, but this method is slow at best, and infeasible for complex geometries. This paper explores an analytical approach to the prediction of percolation threshold in polydisperse mixtures. Specifically, this paper suggests an extension of the concept of excluded volume, and applies that extension to the 2D binary disk system. The simple analytical expression obtained is compared to Monte Carlo results from the literature. The result may be computed extremely rapidly and matches key parameters closely enough to be useful for composite material design.

Published by Elsevier Inc.

1. Introduction

The relationship between transport properties and connectivity is an important application of *percolation theory*, the branch of statistical mechanics concerned with the connectivity of randomly distributed objects. Objects randomly placed into a system may form connected clusters. The onset of percolation occurs when the distributed objects are likely to be part of one connected cluster that spans the entire system.

The bulk properties of a composite material may be strongly influenced by the connectivity of a dispersed particle phase. For example, when the matrix is electrically insulating and the dispersed particles are conductive, connected clusters of particles may create long-range conductive pathways in an otherwise insulating material. When designing a composite material to have a desired set of properties, it may be of interest to find the distribution of particle shapes and sizes that yields, for example, the minimum particle mass fraction to obtain a given resistivity.

Determining the percolation threshold for various arrangements of particles has been the subject of much study in the literature. Berkowitz et al. [1] and Liu et al. [2] offer focused reviews on this topic. In a diverse range of applications, desired bulk material properties appear at the onset of percolation. Such applications include electromagnetic and radio frequency shielding [3,4], thermal resistors and self-regulating heaters [5,6], photothermal optical recording [7], chemical sensors [8], bioelectronics [9], adhesives [10], energetic materials [11], waste stream treatment [12], and functionally customizable

* Corresponding author at: Sandia National Laboratories, Albuquerque, NM 87123, USA.
E-mail address: kmeeks@sandia.gov (K. Meeks).

http://dx.doi.org/10.1016/j.apm.2017.01.046
0307-904X/Published by Elsevier Inc.

Nomenclature

f	= number fraction of smaller disks, i.e. the probability that a randomly selected disk is of the smaller size
n	= inclusion number density, inclusion concentration
r_1	= radius of the larger disk
r_2	= radius of the smaller disk
v	= volume fraction
N	= number of inclusions
R	= radius
η	= inclusion fraction
λ	= disk radius proportionality constant, given by r_2/r_1 such that λ is always less than one
Φ	= fill fraction
$\mathcal{O}$	= set of objects
$\mathcal{V}_{sys}$	= total system measure
$\mathcal{V}$	= measure, used in place of area, A, or volume, V
$\mathcal{V}_{ex}$	= excluded measure
P_{ex}	= pairwise probability of contact
$_{ex}$	= excluded
$_c$	= critical value, the value corresponding to the onset of percolation
$_2$	= system of dimensionality two
$_3$	= system of dimensionality three

polymer composites [13–15]. The application of percolation theory in each of these cases relies on models with highly simplified assumptions relative to the physical system of interest. Although the quantitative predictions used are not wholly accurate, they are still used to guide designs. Improvements to the understanding of percolation theory, particularly for cases which reflect real world systems, can have impact in a wide variety of fields.

Some variables used to describe connectivity in two dimensions include the *total area fraction,* η_2, which is the area of all objects in the system normalized by system size. For disks of radius R with number density n, the total area fraction is defined by

$$\eta_2 = \pi R^2 n. \tag{1}$$

This concept is easily extended to the three dimensional case, where for spheres of radius R with number density n, the *total volume fraction* is given by

$$\eta_3 = \frac{4}{3}\pi R^3 n. \tag{2}$$

The dimension-specific terms of “area” and “volume” make a comprehensive discussion cumbersome. Therefore we adopt the following dimension-independent terminology:

Remark 1. Percolation in two dimensions is closely related to percolation in three dimensions, and except for specific calculations it is most natural to provide a unified treatment. To that end, “measure” is used to mean “area” when the system is two dimensional, and “volume” when the system is three dimensional. The symbol $\mathcal{V}$ is used for the measure, to distinguish it from area, A, or volume, V. Percolation theory may be applied variously to particles distributed over a region, voids in a material, site occupancy in a lattice, bonds between sites, etc. Here we discuss all such cases as spatially distributed “included objects,” or “inclusions.”

We hereafter refer to the inclusion fraction, denoted η, that is the total measure of all included objects normalized by the total system measure. The fill fraction, denoted Φ, is the fraction of the system measure that is occupied by at least one inclusion. The fill fraction is always less than or equal to the inclusion fraction, with equality in the case that the inclusions do not interpenetrate. The inclusion fraction at the onset of percolation is called the critical inclusion fraction, denoted η_c, and the corresponding fill fraction at the onset of percolation is called the critical fill fraction, or percolation threshold, denoted Φ_c.

In 1970, Scher and Zallan demonstrated that the critical inclusion fraction is a universal invariant for lattices occupied by non-interpenetrating monodisperse disks or spheres, dependent only on the dimension of the system [16]. They found that for two-dimensional lattices the critical inclusion fraction is $\eta_{c,2} = 0.45$, regardless of specific lattice geometry, and for three-dimensional lattices the critical inclusion fraction is $\eta_{c,3} = 0.16$. By construction, lattice inclusions do not interpenetrate, so the values for critical fill fractions are the same as for the critical inclusion fractions.

The behavior of engineered composite materials is perhaps more closely related to continuum percolation, in which any of a continuum of points in a system may be occupied [17]. Research suggests that there are also universal percolation thresholds for monodisperse interpenetrating objects in a continuum [18]. Since the inclusions are allowed to interpenetrate,

fill fraction and inclusion fraction differ; critical values may be given in terms of either one, and related to one another as in Section 2 below. Researchers report numerical experiments that give estimates of the critical parameters for disks in two dimensions of $\eta_{c,2} = 1.128$ and $\Phi_{c,2} = 0.67$, and for spheres in three dimensions of $\eta_{c,3} = 0.34$ and $\Phi_{c,3} = 0.28$ [19–21]. Moving beyond disks and spheres requires an extension of the inclusion fraction calculation based on the *excluded region*, which here denotes the set of points such that a second object placed at that point will contact the original object [18]. The *excluded measure* is the measure of the excluded region. Since the excluded region generally depends on the relative orientation of the two objects, the excluded measure is calculated as an expected value over all possible relative orientations. The need for an extended concept of measure can be seen by considering irregular objects like filaments or thin rods. Though these may occupy little or no physical space, it is intuitively clear that they will intersect and connect, and ultimately that these connections will result in percolation. The excluded measure captures the potential for such contact. Numerical studies in two dimensions suggest that the critical excluded inclusion fraction for monodisperse irregular objects is between 3.2 and 4.5 [22]. This result is consistent with the critical physical inclusion fraction of monodisperse disks; as the excluded area of a disk is four times its physical area, the critical excluded inclusion fraction is near the upper bound of this range. The equivalent range in three dimensions, hypothesised by Balberg et al. to be between 0.7 and 2.8 [22], was consistent with extensive Monte Carlo simulations of ellipsoids in three dimensions [23].

Monte Carlo simulations in the literature present percolation threshold values for interpenetrating disks, squares, and sticks of uniform dimension and random distribution [19]. Several researchers have determined the percolation threshold of interpenetrating disks of a single radius using Monte Carlo simulations [19,20]. Researchers have also studied the percolation threshold of interpenetrating disks with two different radii, also called the binary disk system [24,25]. Numerical percolation studies are reported for disks with more than two different radii [26–29], and for the related problems for spheres in three dimensions [30,31]. For the binary disk system it has been reported that the percolation threshold, Φ_c, of any binary disk system is higher than for the monodisperse case [24,25,32]. Specifically, Quintanilla [24] uses Monte Carlo simulations to compute the percolation threshold as a function of the relative concentrations of the two types of disks and the ratio between the large and small disk radii.

The standard definition of excluded measure refers to contact between two identical objects (albeit over a range of relative orientations). Therefore to obtain similar universality estimates for polydisperse systems, the concept of excluded measure must be further generalized. The extension considered here is to apply the previous definition of excluded measure to all possible pairs of objects, and then to find the average over all possible pairs, weighted by the probability that each pairing will occur. We refer to the result as the *average excluded measure*. The average excluded measure evidently reduces to the standard definition in the monodisperse case, where there is only one possible interaction.

The following sections present an estimate for the percolation threshold of binary disk dispersions based on the hypothesis that this average excluded area is invariant at percolation, with the invariant value determined from the monodisperse limiting cases. The resulting analytical expression for the percolation threshold is subsequently compared to previously published Monte Carlo results.

2. Methods

As described in Section 1, the excluded fill fraction has been observed to be roughly invariant for monodisperse systems. This section proposes an extension of the concept of excluded fill fraction to polydisperse systems. We begin with a brief review of existing results for continuum percolation of monodisperse systems of irregular interpenetrating inclusions. We then propose an extension of existing results to polydisperse mixtures. We close the section with the illustration of this extension to the system of bidisperse interpenetrating disks in the plane.

2.1. Number density, fill fraction, excluded measure and percolation threshold

To avoid complications from edge effects, it is convenient to consider percolation in large systems, where the system measure is much larger than that of any individual inclusion. The relationship between number density and fill fraction for interpenetrating inclusions in a large system may be found by the following limiting process as the total system measure becomes large:

Consider a monodisperse system of N interpenetrating inclusions, each of measure $\mathcal{V}$. Let these inclusions be placed in a system of finite measure $\mathcal{V}_{\text{sys}}$. Furthermore, let the system size be chosen based on N so that the inclusion fraction

$$\eta = N\mathcal{V}/\mathcal{V}_{\text{sys}} \tag{3}$$

is constant. The probability that a particular point will be contained within a single inclusion placed into the system is

$$P = \mathcal{V}/\mathcal{V}_{\text{sys}}. \tag{4}$$

The probability that any given point in the system is contained in exactly k inclusions is given by the binomial distribution [33],

$$\mathcal{P}(k; N, P) = \binom{k}{N} P^k (1-P)^{N-k}. \tag{5}$$

By construction, the product $NP = (\eta \mathcal{V}_{\text{sys}}/\mathcal{V}) \cdot (\mathcal{V}/\mathcal{V}_{\text{sys}}) = \eta$ is constant. Therefore the probability $\mathcal{P}(k; N, P)$ as N becomes large is given by the Poisson Limit Theorem [33],

$$\lim_{N\to\infty} \mathcal{P}(k; N, P) = \frac{\eta^k}{k!} e^{-\eta}. \tag{6}$$

The fraction of the system that is not contained in any inclusion is found by setting k to zero; the complement of this value is the fill fraction,

$$\Phi = 1 - e^{-\eta}. \tag{7}$$

As discussed in Section 1, for monodisperse systems of irregular objects the physical fill fraction is replaced by the excluded fill fraction. Specifically, the excluded inclusion fraction η_{ex} is computed by substituting the excluded measure $\mathcal{V}_{\text{ex}}$ in place of the physical measure $\mathcal{V}$ in Eq. (3). Then the excluded fill fraction is given by $\Phi_{ex} = 1 - \exp(-\eta_{ex})$. The invariance of the critical excluded fill fraction means that there is an invariant value $\Phi_{ex,c}$ (or, equivalently, invariant $\eta_{ex,c}$) that predicts the onset of percolation. For monodisperse disks in the plane, the excluded inclusion fraction and the physical inclusion fraction are related by

$$\eta_{ex} = \pi (2R)^2 n = 4\eta_2. \tag{8}$$

Since the two criticality criteria must coincide for this case, $\eta_{ex,c} = 4\eta_{c,2}$.

Use of the excluded measure to characterize the inclusions allows interpretation of the probability P in terms of contact between inclusions:

Remark 2. If a single inclusion is placed randomly into a system, the probability that a randomly selected point will lie within that inclusion is given by $P = \mathcal{V}/\mathcal{V}_{\text{sys}}$. Analogously, the probability that that a randomly selected point will lie within the *excluded region* of the inclusion is $P_{ex} = \mathcal{V}_{ex}/\mathcal{V}_{\text{sys}}$. P_{ex} is also the probability that a second identical inclusion, placed randomly into the system, will penetrate or contact the first. That is, P_{ex} is the probability that two identical inclusions placed into the system with random position and orientation will interpenetrate. We subsequently refer to P_{ex} as the *pairwise probability of contact*.

In practice it is often easier to control the density of inclusions in the system rather than the total number. Therefore we define the *inclusion number density* or *inclusion concentration* as $n \equiv N/\mathcal{V}_{\text{sys}}$. Then, from Eqs. (3) and (4) we obtain the relationship

$$\eta_{ex} = n\mathcal{V}_{\text{ex}} \tag{9}$$

$$= nP_{ex}\mathcal{V}_{\text{sys}}. \tag{10}$$

2.2. Partial excluded measure and pairwise probability of contact

Eq. (9) is useful because it allows the critical inclusion concentration to be predicted in terms of the excluded measure. The standard definition of excluded measure assumes only a single type of object. However the pairwise probability of contact can be well defined for the polydisperse case. Hence we hypothesize that Eq. (10) will hold in general, and we derive our proposed extension below.

For a collection of polydisperse objects, the usual definition of excluded volume can be applied pairwise. Consider a set of inclusion types $\mathcal{O}$. Denote the probability of choosing inclusion O_i from $\mathcal{O}$ as P_i, and assume these probabilities are independent. Let $O_i, O_j \in \mathcal{O}$ be two inclusions. Fix the relative orientation of O_i and O_j, and determine the set of placements for O_j such that contact occurs. Define the *partial excluded measure* $\mathcal{V}_{ij}$ to be the expected value of the measure of this set of points over all possible relative orientations. Note that $\mathcal{V}_{ii}$ is the usual definition of excluded measure for O_i, and that $\mathcal{V}_{ij} = \mathcal{V}_{ji}$. Then the probability P_{ex} that any two inclusions, selected at random and placed into the system with random position and orientation, will be in contact is

$$P_{ex} = \sum_{i,j} P_i P_j \left(\frac{\mathcal{V}_{ij}}{\mathcal{V}_{\text{sys}}} \right) \tag{11}$$

$$= \frac{1}{\mathcal{V}_{\text{sys}}} \sum_{i,j} P_i P_j \mathcal{V}_{ij}. \tag{12}$$

With this expression for P_{ex}, Eq. (10) becomes

$$\eta_{ex} = n\mathcal{V}_{\text{sys}} \frac{1}{\mathcal{V}_{\text{sys}}} \sum_{i,j} P_i P_j \mathcal{V}_{ij} \tag{13}$$

$$= n \sum_{i,j} P_i P_j \mathcal{V}_{ij}. \tag{14}$$

We now state our main hypothesis:

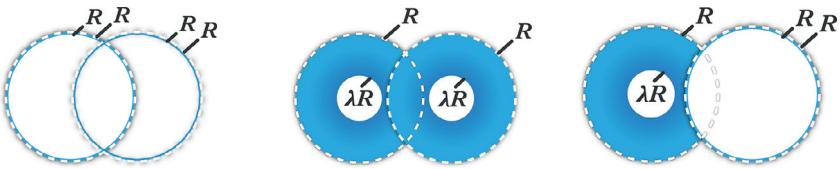

(a) Geometry for computing $\mathcal{V}_{11}$. Both disks of radius r_1

(b) Geometry for computing $\mathcal{V}_{22}$. Both disks of radius r_2

(c) Geometry for computing $\mathcal{V}_{12}$. One disk of radius r_1 and the other of radius r_2

Fig. 1. Each of the mutually exclusive possibilities for inclusion interaction. Geometry for both disks of radius r_1 is shown in (a), both disks of r_2 in (b), and one disk of radius r_1 and the other of radius r_2 in (c). Note that the average excluded area for both disks of r_1 depicted in (a) will be constant. The average excluded area of the pairs depicted in (c) or (b) will be dependent on the value of λ.

Hypothesis 1. For any set $\mathscr{O}$ of N distinct inclusions, let each have a partial excluded measure $\mathcal{V}_{ij}$ as defined above, noting that $\mathcal{V}_{ij} = \mathcal{V}_{ji}$. Let n_i be the number density of the i^{th} inclusion type, let $n = \sum_i n_i$, and let $f_i = n_i/n$. Then the critical value n_c corresponding to the onset of percolation is related to the invariant quantity $\eta_{ex,c}$ by

$$\eta_{ex,c} = n_c \sum_{i,j} f_i f_j \mathcal{V}_{ij}. \tag{15}$$

2.3. Percolation threshold for the 2D binary disk system

We now apply Eq. (15) to a 2D system comprising disks with two possible values for their radius. The larger disk type, O_1, has radius $r_1 = R$, and the smaller disk type, O_2 radius $r_2 = \lambda R$, where $0 < \lambda < 1$. The relative number fraction n_2/n of smaller disks is $f_2 = f$ and therefore the relative number fraction n_1/n of larger disks is $f_1 = 1 - f$. While there are many other interesting distributions, this system is chosen for explicit computation because extensive Monte Carlo simulation results are available for comparison. As will be seen below, the results suggest further modification to the notion of partial excluded measure.

The three distinct partial excluded areas are $\mathcal{V}_{11}$, $\mathcal{V}_{12}$, and $\mathcal{V}_{22}$. The corresponding contact geometries are depicted in Fig. 1. The partial excluded area for each case can be written as a function of R and λ.

$$\mathcal{V}_{11} = 4\pi R^2 \tag{16}$$

$$\mathcal{V}_{12} = \pi (1+\lambda)^2 R^2 \tag{17}$$

$$\mathcal{V}_{22} = 4\pi \lambda^2 R^2 \tag{18}$$

Substituting these values, and the values for f_1 and f_2, into Eq. (15) gives

$$\eta_{ex,c} = 2n_c \pi R^2 \left[2(1-f)^2 + (1-f)f(1+\lambda)^2 + 2f^2\lambda^2\right] \tag{19}$$

Simplifying this gives

$$\eta_{ex,c} = 2n_c \pi R^2 \left[(\lambda-1)^2 f^2 + (\lambda-1)(\lambda+3)f + 2\right] \tag{20}$$

We may use this relationship to compute the critical number density n_c given R, f, and λ,

$$n_c = \frac{\eta_{ex,c}}{2\pi R^2} \frac{1}{\left[(\lambda-1)^2 f^2 + (\lambda-1)(\lambda+3)f + 2\right]}. \tag{21}$$

We may compute the *physical* inclusion fraction for the binary disks of any number density n by

$$\eta = \pi R^2 n \left[f\lambda^2 + 1 - f\right]. \tag{22}$$

By Eq. (7), we can write the physical fill fraction for such systems as

$$\Phi = 1 - \exp\left(-\pi R^2 n \left[f\lambda^2 + 1 - f\right]\right) \tag{23}$$

At percolation, Eqs. (23) and (21) give the percolation threshold Φ_c in terms of f and λ as

$$\Phi_c = 1 - \exp\left(-\frac{\eta_{ex,c}\left[f\lambda^2 + (1-f)\right]}{2\left[(\lambda-1)^2 f^2 + (\lambda-1)(\lambda+3)f + 2\right]}\right) \tag{24}$$

Eq. (21) may be checked explicitly for four degenerate cases in which the bidisperse system reduces to the monodisperse case. For $f = 0$ and $f = 1$, the system contains either all large or all small disks. From Eq. (19) it is clear that the correct

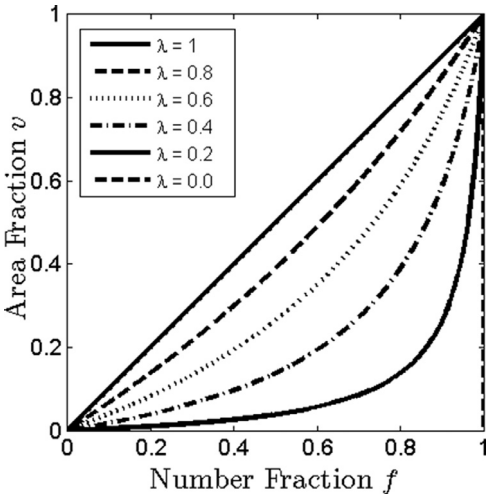

Fig. 2. Plot of $v_\lambda(f)$ versus f given by Eq. (26). The curves coincide when $\lambda = 1$ and for the points $f = 0$ and $f = 1$. Otherwise $v_\lambda(f)$ is strictly less than f.

limits are obtained as, respectively, $n_c = \eta_{ex,c}/4\pi R^2$ and $n_c = \eta_{ex,c}/4\pi\lambda^2 R^2$. The case $\lambda = 1$ also reduces to monodisperse disks of radius R, and we again obtain $n_c = \eta_{ex,c}/4\pi R^2$, as expected.

The case $\lambda = 0$ is instructive, and reveals a deficiency in the direct application of the definition of excluded measure as inherited from the monodisperse case. Setting the radius of the smaller disks to zero effectively removes them from the system. Hence the expected critical concentration is the monodisperse formula for large disks, but with n_c replaced by $(1-f)n_c$ to reflect the lower effective concentration of large disks. That is, we expect the result $(1-f)n_c = \eta_{ex,c}/4\pi R^2$. However, Eq. (19) instead returns

$$(1-f)n_c = \frac{\eta_{ex,c}}{4\pi(1-f/2)R^2}. \tag{25}$$

The reason for the unexpected term $(1-f/2)$ can be seen in the expression $\mathcal{V}_{12}$. If the small disks were removed from the system, then both partial excluded areas involving the smaller disks, namely $\mathcal{V}_{12}$ and $\mathcal{V}_{22}$, would be zero. However when λ is set to zero in Eq. (17), $\mathcal{V}_{12}$ is not zero, but πR^2. The reason for this is physically clear: the calculation is accounting for the contact that occurs between the infinitesimally small disks contained within the area of the larger disk. Because the small disks occupy no space, and are completely contained within the area of the larger disk, this contact does not lead to the growth of clusters of inclusions, and therefore cannot contribute to percolation. Therefore this term represents a gap in the link between contact and percolation, which only becomes apparent when the disks are of greatly different sizes. Several approaches suggest themselves for correcting this effect, including explicitly removing configurations where one object is completely contained within the other, or weighting the various configurations by the amount the measure increases over a single inclusion. Exploring these ideas is of great interest, but a comprehensive study is beyond the scope of the current paper. Below we present a heuristic correction to Eq. (24) and consider the result.

Consider the area fraction of the smaller disks, given by

$$v_\lambda(f) = \frac{f\lambda^2}{f\lambda^2 + (1-f)}. \tag{26}$$

The quantity $v_\lambda(f)$ is the area of the small disks divided by the area of all disks in the system and takes values between zero and one. It is equal to zero when f is equal to zero and equal to one when f is equal to one, and will be strictly less than f for any other value. The difference becomes greater as λ becomes smaller, approaching a step function as λ approaches zero. Fig. 2 plots $v_\lambda(f)$ versus f for various values of λ.

As argued above, Eq. (24) overstates the contribution of the smaller disks to percolation when the radius ratio λ is small. Substituting $v_\lambda(f)$ for f incorporates a "size correction factor" to offset the effects of spurious contacts that do not contribute to percolation. That substitution yields corrected expressions for Φ_c, as follows:

$$\Phi_c' = 1 - \exp\left(-\frac{\eta_{ex,c}\left[v_\lambda(f)\lambda^2 + (1-v_\lambda(f))\right]}{2[(\lambda-1)^2 v_\lambda(f)^2 + (\lambda-1)(\lambda+3)v_\lambda(f) + 2]}\right), \tag{27}$$

where $v_\lambda(f)$ is given by Eq. (26). The substitution of $v_\lambda(f)$ for f in Eq. (24) to yield Eq. (27) is not a general substitution of $v_\lambda(f)$ for f, but rather a volume weighting that only applies to prediction of the percolation threshold. This substitution effectively weights the predicted contribution of the smaller disks to the onset of percolation by the ratio of the disk areas, λ. In particular, Φ_c' can be used to calculate the predicted critical density from Eq. (23). When λ is zero, $v_\lambda(f)$ is also zero,

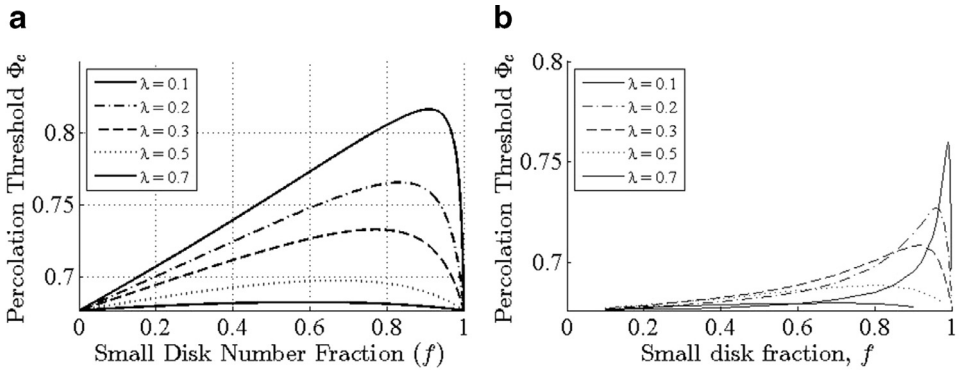

Fig. 3. Comparison of the percolation threshold,Φ_c, from Eq. (24) in (a) and Quintanilla [24] in (b) for $\lambda = 0.1, 0.2, 0.3, 0.5, 0.7$ in (b).

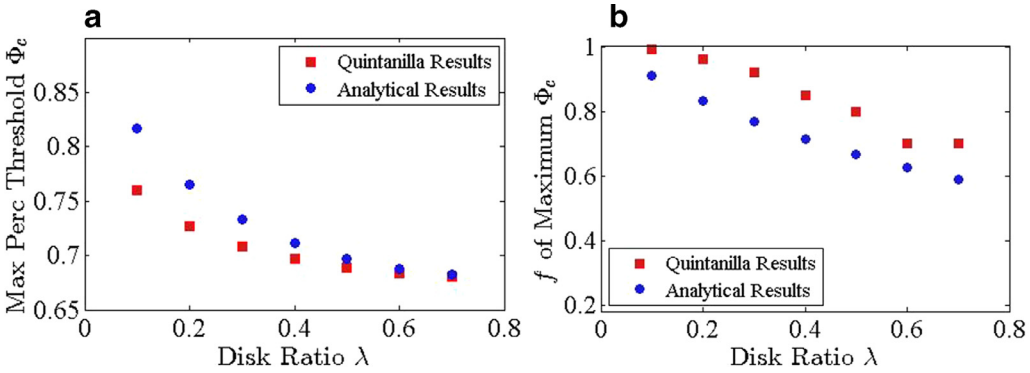

Fig. 4. Comparison of simulated and computed maximum values of η_c (a), and simulated and computed location of maximum η_c for a give f (b). Relatively good matching of computed and previously published results is observed.

and the predicted critical disk density is $(1-f)n_c' = \eta_{ex,c}/4\pi R^2$. Thus this substitution appears to satisfy the heuristic more fully, as it recovers the factor $(1-f)$.

3. Results

Fig. 3a plots Φ_c as computed from Eq. (24) versus f for various values of λ. Fig. 3b shows the percolation threshold of binary dispersions for varying f and λ from Quintanilla [24].

While Eq. (24) does not give the exact dependence of Φ_c on f seen in the Monte Carlo simulations, some key design parameters do show reasonable agreement. Fig. 4a compares the maximum percolation threshold as a function of λ. The values agree to within seven percent. Fig. 4b compares plots for the value of f that gives the maximum value of Φ_c, as a function of λ. These curves also show reasonable agreement, although there are limited data available from the Monte Carlo results.

The hypothesis that $\eta_{ex,c}$ is invariant can be checked from the Monte Carlo results of [24]. Rearranging Eq. (24) to Eq. (28) allows $\eta_{ex,c}$ to be calculated on a case by case basis as,

$$\eta_{ex,c} = \frac{\left[(\lambda-1)^2 f^2 + (\lambda-1)(\lambda+3)f + 2\right]2\eta_c}{[f\lambda^2 + 1 - f]}. \tag{28}$$

Fig. 5 plots $\eta_{ex,c}$ as a function of f and λ based on the preceding analysis. The results show that $\eta_{ex,c}$ is, in fact, not constant for the Monte Carlo simulations in [24], although the values range between 3.1 and 4.5, which is comparable to the critical excluded area range of 3.2 to 4.5 observed for monodisperse, irregularly shaped planar objects [18]. We note that the calculations above include the spurious contacts due to completely contained objects, and these results may be improved by modified contact models.

Fig. 6a shows Φ_c' plotted against f, with the comparison Monte Carlo results [24] shown in Fig. 6b. The qualitative similarity between the curves is noteworthy. The peak values predicted by Eq. (24) are equal to the peak values predicted by Eq. (27), and thus the comparison presented in Fig. 4a is true of Eq. (27) as well as Eq. (24). The locations of these peaks, however, are not the same. A comparison of the locations of the maximum percolation threshold values predicted by Eq. (27) to the published [24] results is shown in Fig. 7. The location of the prediction of the peak is much closer to the published

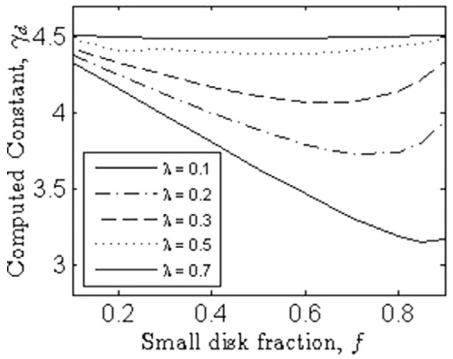

Fig. 5. Calculated value of $\eta_{ex,c}$ from the Monte Carlo results published by Quintanilla [24] using equation Eq. (28). This value is variable as a function of both f and λ, contrary to the expectations of our hypothesis.

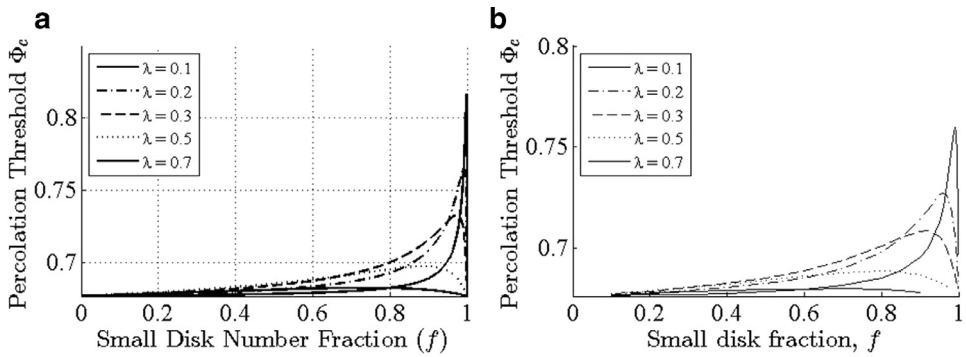

Fig. 6. The percolation threshold as a function of f and λ, as determined from (27) are shown in (a). This graph is qualitatively similar to published results from [24], shown in (b).

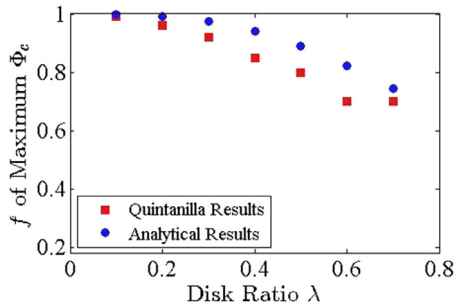

Fig. 7. The value of the small disk fraction f, resulting in the maximum value of percolation threshold, Φ_c, for a given value of λ from the published [24] results, as well as from Eq. (27).

result. Thus, even though this formulation does not capture aspects of the monodisperse case, it seems a more promising starting point for future exploration.

Remark 3. Eq. (15) assumes that the particle classes are drawn from discrete classes, however the hypothesis may be extended to systems with continuous distributions of particle classes. Consider a system of disks, each of which has a radius drawn from a probability density $f(R)$ such as the Weibull or log-normal distribution. Then the critical value n_c corresponding to the onset of percolation would be related to the invariant quantity $\eta_{ex,c}$ by

$$\eta_{ex,c} = n_c \int_0^\infty \int_0^\infty f(R_i) f(R_j) \mathcal{V}(R_i, R_j)\, dR_i\, dR_j. \tag{29}$$

For disks $\mathcal{V}(R_i, R_j) = \pi \left(R_i + R_j\right)^2$ is the excluded area of the contact pair given by R_2 and R_1.

4. Discussion

The preceding results suggest that while $\eta_{ex,c}$ is not invariant for the binary disk system, the expressions resulting from an assumption of approximate invariance may be sufficient for material design purposes. It is relevant to note here that this analytical expressions can be manipulated algebraically and evaluated almost instantly, while the Monte Carlo results used for comparison required many weeks of computation to obtain [24].

The assumption of constant average excluded measure used in the derivation of Eq. (24) includes spurious contacts between the large disks and completely contained smaller disks, even though these contacts do not increase the effective size of the cluster. The heuristic modifications resulting in Eq. (27) weight the contribution of smaller disks in proportion to their area, thus reducing the impact of these spurious contacts. The striking improvement due to this adjustment validates the overall approach, and suggests that analytical models giving close agreement are not out of the question.

5. Conclusion

In this work we presented an easily computed analytical expression for estimating the percolation threshold for a system with disks of two different radii. The percolation theory for the uniform disk system was extended based on the heuristic that the average excluded measure at percolation will be constant. Comparison to previously published Monte Carlo simulations show reasonable agreement of key parameters. This level of accuracy would be sufficient for many design tasks, especially considering the many deviations of a real material system from the geometric ideal. Slight adjustments in the analytical model yield striking similarity to the Monte Carlo results. Exploring further improvements to this heuristic is a topic of our current research.

Acknowledgments

Sandia National Laboratories is a multi-program laboratory managed and operated by Sandia Corporation, a wholly owned subsidiary of Lockheed Martin Corporation, for the U.S. Department of Energys National Nuclear Security Administration under contract DE-AC04-94AL85000. This document has been reviewed and approved for unclassified, unlimited release.

The authors are grateful for support from the Army Research Office contract number W911NF-14-1-0250 and encouragement from our program manager, Dr. Ralph Anthenien. K. Meeks would like to thank Casey Webb, for her assistance with graphics, and Dr. John Tencer for his insights during the editing process. J. M. Berg was supported by the National Science Foundation.

References

[1] B. Berkowitz, R. Ewing, Percolation theory and network modeling applications in soil physics, Surv. Geophys. 19 (1998) 23–72.
[2] J. Liu, K. Regenauer-Lieb, Application of percolation theory to microtomography of structured media: percolation threshold, critical exponents, and upscaling, Phys. Rev. E Stat. Nonlinear Soft Matter Phys. 83 (1) (2011) 37–43.
[3] M. Zeng, D. Zhao, R. Yu, M. Feng, B. Yang, X. Liu, Y. Zhang, X. Wang, Low percolation threshold carbon-black/nitrile-butadiene-rubber composites and their electromagnetic shielding effects, J. Nanosci. Nanotechnol. 13 (2) (2011) 1339–1342.
[4] L. Nayak, T.K. Chaki, D. Khastgir, Electrical percolation behavior and electromagnetic shielding effectiveness of polyimide nanocomposites filled with carbon nanofibers, J. Appl. Polym. Sci. 131 (24) (2014).
[5] C. Pennetta, L. Reggiani, L. Kiss, Thermal effects on the electrical degradation of thin film resistors, Phys. A Stat. Mech. Appl. 266 (1–4) (1999) 214–217.
[6] A. Snarskii, A. Dziedzic, B.W. Licznerski, Temperature behavior of percolation and percolation-like systems, Int. J. Electron. 81 (4) (1996) 363–370.
[7] M. Ibrahim, M. Bassil, U.B. Demirci, T. Khoury, G.E.H. Moussa, M.E. Tahchi, P. Miele, Polyaniline-Titania solid electrolyte for new generation photovoltaic single-layer devices, Mater. Chem. Phys. 133 (2–3) (2012) 1040–1049.
[8] C. Li, E. Thostenson, T.-W. Chou, Sensors and actuators based on carbon nanotubes and their composites: a review, Compos. Sci. Technol. 68 (2008) 1227–1249.
[9] M. Yang, S. Sun, H.A. Bruck, Y. Kostov, Rasooly, Electrical percolation-based biosensor for real-time direct detection of staphylococcal enterotoxin b (SEB), Biosens. Bioelectron. 25 (12) (2010) 2573–2578.
[10] H. Wu, X. Wu, M. Ge, G. Zhang, Y. Wang, J. Jiang, Effect analysis of filler sizes on percolation threshold of isotropical conductive adhesives, Compos. Sci. Technol. 67 (6) (2007) 1116–1120.
[11] E. Collins, B. Skelton, M. Pantoya, F. Irin, M. Green, M. Daniels, Effect analysis of filler sizes on percolation threshold of isotropical conductive adhesives, composites science and technology, Combust. Flame 162 (4) (2015) 1417–1421.
[12] N. Yoshikawa, K. Kawahira, Y. Saito, H. Todoroki, S. Taniguchi, Estimation of microwave penetration distance and complex permittivity of graphite by measurement of permittivity and direct current conductivity of graphite powder mixtures, J. Appl. Phys. 117 (2015) 084105.
[13] F. Irin, S. Das, F.O. Atore, M.J. Green, Ultralow percolation threshold in aerogel and cryogel templated composites, Langmuir 29 (2013) 11449–11456.
[14] J. Grunlan, W. Gerberich, L. Francis, Lowering the percolation threshold of conductive composites using particulate polymer microstructure, J. Appl. Polym. Sci. 80 (2001) 692–705.
[15] K. Kalaitzidou, H. Fukushima, L.T. Drzal, A new compounding method for exfoliated graphitepolypropylene nanocomposites with enhanced flexural properties and lower percolation threshold, Compos. Sci. Technol. 67 (2007) 2045–2051.
[16] H. Scher, R. Zallen, Critical density in percolation processes, J. Chem. Phys. 53 (9) (1970) 3759–3761.
[17] S. Lee, S. Torquato, Monte carlo study of correlated continuum percolation: universality and percolation thresholds, Phys. Rev. A. 41 (10) (1990) 5338–5344.
[18] I. Balberg, C. Anderson, S. Alexander, N. Wagner, Excluded volume and its relation to the onset of percolation, Phys. Rev. B 30 (7) (1984) 3933–3943.
[19] S. Mertens, C. Moore, Continuum percolation thresholds in two dimensions, Phys. Rev. E 86 (6) (2012) 061109.
[20] J. Quintanilla, S. Torquato, R. Ziff, Efficient measurement of the percolation threshold for fully penetrable discs, J. Phys. A Math. General 399 (42) (2000) 399–407.
[21] E. Gawlinski, H. Stanley, Continuum percolation in two dimensions: Monte Carlo tests of scaling and universality for non-interacting discs, J. Phys. A.: Math. General 14 (8) (1981) L291–L299.

[22] I. Balberg, Universal percolation-threshold limits in the continuum, Phys. Rev. B 31 (6) (1985) 4053–4055.
[23] E. Garboczi, K. Snyder, J. Douglas, M. Thorpe, Geometrical percolation threshold of overlapping ellipsoids, Phys. Rev. E 52 (1) (1995) 819–828.
[24] J. Quintanilla, Measurement of the percolation threshold for fully penetrable disks of different radii, Phys. Rev. E 63 (6) (2001) 061108.
[25] A. Balram, D. Dhar, Scaling relation for determining the critical threshold for continuum percolation of overlapping discs of two sizes, Pramana J. Phys. 74 (1) (2010) 109–114.
[26] A. Gervois, C. Annic, J. Lemaitre, M. Ammi, Arrangement of discs in 2d binary assemblies, Phys. A Stat. Mech. Appl. 218 (1995) 403–418.
[27] J. Quintanilla, R. Ziff, Asymmetry in the percolation thresholds of fully penetrable disks with two different radii, Phys. Rev. E 76 (5) (2007) 051115.
[28] V. Sasidevan, Continuum percolation of overlapping disks with a distribution of radii having a power-law tail, Phys. Rev. E 88 (2013) 022140.
[29] M. Phani, D. Dhar, Continuum percolation with discs having a distribution of radii, J. Phys. A Math. General 645 (1984).
[30] R. Consiglio, D. Baker, G. Paul, H. Stanley, Continuum percolation thresholds for mixtures of spheres of different sizes, Physica Stat. Mech. Appl. 319 (2003) 49–55.
[31] D. Dhar, On the critical density for continuum percolation of spheres of variable radii, Phys. Stat. Mech. Appl. 242 (1997) 341–346.
[32] D. He, N. Ekere, L. Cai, Two-dimensional percolation and cluster structure of the random packing of binary disks, Phys. Rev. E 65 (6) (2002) 061304.
[33] J.W. Harris, H. Stocker, The Handbook of Mathematics and Computational Science, Springer-Verlag New York, Inc., Secaucus, NJ, 1997.